Radiative slowing down and monochromatization of a beam of sodium atoms in a counterpropagating laser beam

S. V. Andreev, V. I. Balykin, V. S. Letokhov, and V. G. Minogin

Institute of Spectroscopy, Academy of Sciences of the USSR, Troitsk, Moscow Province
(Submitted 10 November 1981)
Zh. Eksp. Teor. Fiz. **82**, 1429–1441 (May 1982)

An experimental investigation was made of the slowing down of a thermal beam of sodium atoms by counterpropagating resonance laser radiation. Direct determination of the distribution of the longitudinal atomic velocities was used to study the velocity monochromatization of the atomic beam. A comparison of the experimental and theoretical results was made. For the effective slowing down length of 20 cm in our experiments the narrowing of the distribution of the longitudinal velocities was nineteen-fold and this corresponded to lowering of the temperature of the relative motion of atoms to 1.5 °K.

PACS numbers: 32.80. – t, 07.77. + p

1. INTRODUCTION

Considerable attention is being given currently to the problem of the interaction of resonance laser radiation with the translational state of atomic particles. One of the main reasons for this interest is the attempt to develop methods for controlling spatial motion of atoms with the aid of resonance optical pressure. In particular, experiments have been reported on the deflection,[1,2] control of the transverse width,[3,4] and control of the longitudinal velocity (slowing down)[5,6] of atomic beams (see also a review in Ref. 7).

Among the various methods of controlling the motion of atoms, that of the greatest practical interest is the radiative slowing down of atomic beams which makes it possible to form monochromatic beams of slow atoms or ensembles of atoms with zero average velocity and temperature well below the room value.

According to theoretical estimates,[8,9] the maximum width of the distribution of longitudinal velocities in an atomic beam is given by the expression $\delta v \approx (\hbar\gamma/M)^{1/2}$, where 2γ is the radiative width of a transition and M is the mass of an atom. For example, in the case of sodium atoms we have $\delta v \approx 40$ cm/sec. Further monochromatization of an atomic beam is hindered by the diffusion spreading of atoms in the velocity space, which is due to the random nature of the optical pressure force. Near the turning point of an atom being slowed down the width of the velocity distribution[10,11] reaches $\Delta v = (\hbar|\Omega|/M)^{1/2}$, where $\Omega = \omega - \omega_0$ is the detuning of the frequency of an optical wave ω from the frequency of an atomic transition ω_0. In particular, if the detuning is $\Omega = -k\bar{v}$, where $k = 2\pi/\lambda$ is the wave vector of a wave and $\bar{v}$ is the average thermal velocity of atoms in the original beam (i.e., when a light wave resonates with the majority of atoms), the width of the initial velocity distribution $\Delta v_{in} \approx \bar{v}$ can be reduced to $\Delta v_{fin} \approx (\hbar k\bar{v}/M)^{1/2}$ corresponding to the degree of monochromatization

$$\mu = \Delta v_{in}/\Delta v_{fin} \approx (M\bar{v}/\hbar k)^{1/2} \approx 10^2.$$

Such a high degree of monochromatization corresponds to a reduction in the effective temperature of atoms to values

$$T_{fin} = T_{in}/\mu^2 \approx 10^{-4} T_{in} \approx 10^{-1} - 10^{-2}\ \text{K}.$$

We have reported earlier[5,6] the first experiments on which we observed radiative slowing down and monochromatization of a beam of sodium atoms by cw laser radiation. In the present study we used an improved experimental technique to study directly the narrowing of the velocity distribution in a beam of sodium atoms and attainment of a degree of monochromatization amounting to $\mu \approx 19$.

2. METHOD FOR INVESTIGATING THE DEFORMATION OF THE VELOCITY DISTRIBUTION

We selected the basic experimental configuration (Fig. 1) in which a thermal beam of sodium atoms was irradiated by two counterpropagating laser beams. One of them (a strong laser beam) deformed the atomic velocity distribution. The frequency of this laser beam was constant and it was set within the limits of an absorption line of the atomic beam. The deformation of the atomic velocity distribution in the course of propagation of atoms inside the strong laser beam had the form shown qualitatively in the lower part in Fig. 1. A second weak laser beam was used as the probe. The frequency of the second beam could be tuned within the absorption line profile and a fluorescence signal due to the excited atoms could be recorded simultaneously. Since the signal of the atoms excited by the weak beam was proportional to the number of atoms with a specific velocity projection, this method made it possible to

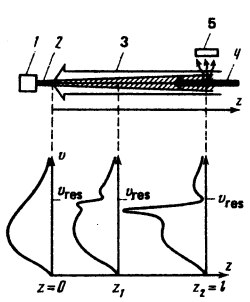

FIG. 1. General experimental configuration and qualitative nature of the deformation of the velocity distribution for an atomic beam irradiated by a counterpropagating resonance light wave. The resonance velocity of atoms is $v_{res} = \Omega/k$ [1) atomic beam source, 2) atomic beam, 3) strong laser beam, 4) probe laser beam, 5) detector].

 0038-5646/82/050828-07$04.00

record directly the longitudinal-velocity distribution of the atoms in the beam. Interference between the fluorescence signal from the strong laser beam with that of the weak fluorescence signal due to the probe beam was avoided by interrupting the strong laser beam periodically with a mechanical chopper and recording the fluorescence only at the time when the strong beam was stopped. During that time all the excited atoms returned to the ground state and the distribution of the velocities in this state was determined by the probe laser beam.

It should be stressed particularly that the weak probe beam did not saturate the resonance transition so that the fluorescence signal due to this beam (when the strong beam was stopped) was directly proportional to the number of atoms with a specific velocity projection in the lower state, i.e., it was proportional to the velocity distribution function of the atoms $w(v)$. In the presence of the strong field it would have been impossible to determine the velocity distribution from the fluorescence signal for two reasons. Firstly, it would be difficult to identify the fluorescence signal due to the probe beam against the background of the fluorescence excited by the strong beam. Secondly, even after separation of the fluorescence excited by the weak beam, it could not be used to determine the real velocity distribution of the atoms but that in the lower state which had a wide Bennett dip due to the excitation of some of the atoms by the strong laser field.

The pulses of the strong beam and the intervals of observation of the fluorescence excited by the weak beam were in the following sequence. The repetition period of the strong beam pulses was $T=170$ μsec (Fig. 2a). The weak beam was operating continuously, but the fluorescence signal due to this beam was recorded 30 μsec after the stoppage of the strong beam. This delay was considerably greater than the spontaneous decay time $\tau_{sp}=16$ nsec and made sure that the fluorescence signal was indeed due to the weak beam. The time taken to record the fluorescence due to the weak beam was 40 μsec, selected to be short compared with the average transit time of atoms ($T_{tr}=0.5$ msec)

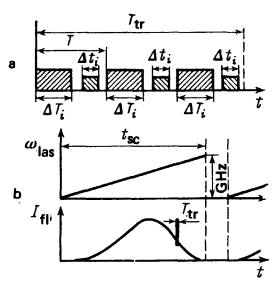

FIG. 2. Time sequence of the irradiation of atoms with a strong beam and of the recording of fluorescence due to a weak beam (a) and the nature of scanning of the absorption profile by the weak probe beam (b). $T_{tr}=0.5$ msec is the average transit time of an atom across the interaction zone; $T=170$ μsec is the chopping period of a modulator (15 in Fig. 5), $\Delta T_i=85$ μsec are the time intervals between the switching on of the strong laser field; $\Delta t_i=40$ μsec are the time intervals during which the fluorescence signal is recorded, $t_{sc}=45$ msec is the duration of the scanning of the frequency of the probe laser radiation.

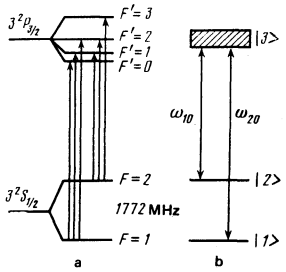

FIG. 3. a) Hyperfine structure of the ground $3S_{1/2}$ and excited $3P_{3/2}$ states of the sodium atom and resonance transitions in the case of two-frequency excitation of the atoms with laser radiation. b) Equivalent three-level scheme used in calculations of the redistribution of the atomic velocities.

through the interaction region $l=40$ cm long. The frequency of the probe beam was scanned linearly with time in the region of 5 GHz and the total scanning time was $t_{sc}=45$ msec [Fig. 2(b)]. The rate of scanning of the probe beam frequency could be varied in the range 90–110 MHz/msec. At this scanning rate the frequency of the weak beam shifted by 16 MHz in the time between two successive fluorescence measurement intervals and the shift was considerably less than the characteristic scale of the deformation of the velocity distribution.

The sodium atom with the $3S_{1/2}-3P_{3/2}$ resonance transition was selected; its ground state was known to be split into two hyperfine structure sublevels and special measures were taken to ensure reliable excitation of atoms from both $F=1$ and 2 states [Fig. 3(a)]. The strong laser radiation was of two-mode nature and the frequency difference between the modes was $\Delta\nu=1772$ MHz. One of the modes excited sodium atoms as a result of the $3S_{1/2}(F=1)-3P_{3/2}$ transition and the other as a result of $3S_{1/2}(F=2)-3P_{3/2}$ [Fig. 3(b)].

The use of a two-frequency optical field could, in principle, alter the above simple pattern of deformation of the velocity distribution, because two light waves could act on different groups of atoms. However, at the temperatures of the atomic beam source employed in the present study the overlap of the absorption lines due to the $3S_{1/2}(F=1)-3P_{3/2}$ and $3S_{1/2}(F=2)-3P_{3/2}$ transitions could be ignored [Fig. 4(a)]. In view of this, the low-frequency mode of the laser radiation of frequency ν_{L1} excited only the atoms from the $F=2$ state,

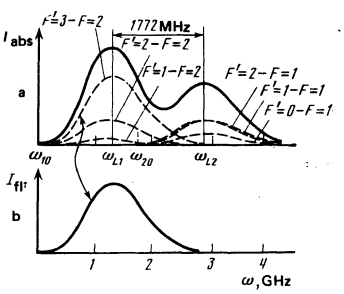

FIG. 4. a) Absorption spectra of a beam of sodium atoms corresponding to the $3S_{1/2}(F=1)-3P_{3/2}$, $3S_{1/2}(F=2)-3P_{3/2}$ transitions and the positions of the laser radiation modes of frequencies ν_{L1} and ν_{L2}. b) Fluorescence profile of atoms in the recording zone.

whereas the high-frequency mode $\nu_{L2}=\nu_{L1}+1770$ MHz excited in practice only the atoms from the $F=1$ state. Since, moreover, the frequency interval between the modes $\nu_{L2}-\nu_{L1}$ was identical with the difference between the frequencies of two resonance transitions $\nu_{20}-\nu_{10}=1772$ MHz, both modes acted on the same velocity group of atoms and they deformed the velocity distributions at the $F=1$ and 2 levels in the same wave.

We shall now consider the expected dependence of the fluorescence intensity on the frequency of the probe field. Since the probe beam could be absorbed as a result of all six allowed transitions between the $3S_{1/2}$ and $3P_{3/2}$ states [Figs. 3(a) and 4(a)], we could generally expect the combined fluorescence profile to repeat the complex combined profile of the absorption line. In the case of a weak deformation of the velocity distribution (for example, in the case of a low intensity of the strong laser beam) we could expect the fluorescence profile to have the form shown in Fig. 4. In the case of a strong deformation of the velocity distribution the fluorescence profile should include six peaks of the type shown in Fig. 1, because the combined fluorescence profile should be due to six shifted velocity distributions.

The interpretation of the results was simplified by selecting such a regime of the excitation by the probe beam which made it possible to observe the fluorescence due to the excitation of atoms solely as a result of $F=2-F'=3$ transition. The probe beam was located entirely inside the region of the interaction between the strong beam and the atomic beam, the polarization of the probe beam was linear, and its frequency was always scanned to the high-frequency part of the absorption line. Under these conditions the optical pumping caused by the probe beam generated fluorescence by excitation of atoms due to the $F=2-F'=3$ transition and the intensity of the fluorescence was over two orders of magnitude higher than the intensity due to the remaining possible transitions, i.e., the fluorescence consisted of just one profile out of the six possible [Fig. 4(b)].

3. APPARATUS

The apparatus used to investigate the velocity monochromatization is shown in Fig. 5. It consisted of the following main components: a two-frequency cw dye laser 2; a one-frequency cw dye laser 1 acting as the probe; an argon (Ar^+) laser which was used as the pump source for the dye lasers; a vacuum chamber 3 with sources of the main 4 and reference 5 atomic beams; a system for recording the fluorescence signal; a system 13 for scanning the frequency of the probe laser; a control cell 16 with sodium vapor and a system for control of the strong laser frequency and of the scanning of the weak laser. Mechanical choppers 14 and 15 ensured periodic interruption of the strong laser radiation.

The strong laser radiation was generated in the two-frequency dye laser 2 and the separation between the emission frequencies was equal to the separation between the components of the hyperfine structure of the

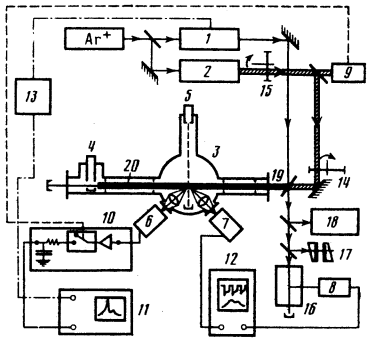

FIG. 5. Schematic diagram of the apparatus: 1) single-mode probe laser; 2) two-frequency strong laser; 3) vacuum chamber; 4), 5) sources of the main and reference atomic beams; 6)–9) photomultipliers; 10) Boxcar integrator; 11), 12), oscilloscopes; 13) frequency scanning module; 14), 15) mechanical choppers; 16) cell with sodium vapor; 17) Fabry-Perrot etalon; 18) spectrometer; 19) semitransparent mirror; 20) zone of interaction between the atomic and laser beams.

ground state of the sodium atom $\Delta\nu_{hfs}=1772$ MHz. This type of emission from the dye laser was achieved as follows. The optical length of the laser resonator was selected so that the separation between the hyperfine structure components of the ground state of the sodium atom was a multiple of the separation between the frequencies of the neighboring axial modes of the laser resonator: $\Delta\nu_{mode}=\Delta\nu_{hfs}/m$, where $m=1,2,3,\ldots$. The experimental values were $\Delta\nu_{mode}=443$ MHz and $m=4$. Use of three Fabry–Perot etalons inside the resonator with free spectral ranges $\Delta\nu_1=85\,000$ GHz, $\Delta\nu_2=1000$ GHz, and $\Delta\nu_3=75$ GHz made it possible to reduce the width of the laser emission spectrum to 2 GHz. Separation, out of the four to six emitted axial modes, of two modes separated by $\Delta\nu_{hfs}=1772$ MHz and suppression of the remaining modes was achieved by utilizing the effect of spatial depletion of inversion.[12] The emission frequency of the two-mode laser was tuned by inclining the intracavity etalons and the fine tuning was in discrete steps equal to the separation between the axial modes; this was done using the etalon with $\Delta\nu_3=75$ GHz. In the adopted resonator configuration the stability of the two-frequency emission spectrum was satisfactory, but tuning of a pair of axial modes over an interval comparable with the Doppler width of the absorption line required synchronous variation of the free spectral range of two etalons ($\Delta\nu_2$ and $\Delta\nu_3$), which was a difficult task.

Single-mode scanning radiation was generated by a Spectra Physics laser model 580A. The beams from both lasers were combined by a system of rotatable mirrors and one semitransparent mirror 19; they were then directed to a vacuum chamber containing the atomic beam sources. The main atomic beam was directed opposite to both laser beams. The aperture of the main atomic beam was governed by a set of slits and its minimum size was greater than the diameter of the laser beams, so that the zone of interaction of the laser beams with the main atomic beam was governed by the aperture of the laser beams. The diameter of the strong laser beam near the exit aperture of the

atomic source was $d'_s = 1.1$ mm and in the recording region it was $d''_s = 1.3$ mm; the corresponding diameters of the probe beam were $d'_p = 0.65$ mm and $d''_p = 0.6$ mm; the probe beam was located inside the strong beam throughout the interaction zone. The length of this zone was 40 cm.

Better spatial coincidence of the atomic and laser beams was ensured by a through exit aperture of the atomic beam source so that the passage of the laser beams through this aperture corresponded automatically to a good spatial coincidence of all three beams. The exit window of the chamber was separated by 32 cm from the recording zone (and at a distance of 72 cm from the atomic beam source), so as to avoid evaporation of a resonance sodium mirror on this window; such a mirror could have reflected strongly the laser radiation. The chamber was evacuated to a pressure of $(3-5)\times 10^{-6}$ Torr. The reference atomic beam was perpendicular to the laser beams and was used to calibrate the frequency scale.

In our experiments the probe laser radiation was switched on continuously and its frequency was scanned along the absorption line profile of the atomic beam. The two-frequency strong laser radiation was modulated by a mechanical chopper 15 and the off-duty factor was 1 : 1 (Fig. 2). The fluorescence due to the probe radiation was recorded only at the moments when the strong field was switched off and a Model 162 Boxcar Integrator was used (10).

The function of the integrator was to switch on the recording apparatus for a certain time interval when the strong field was switched off. The time constant of the recording apparatus ($\tau = 0.5$ msec) was greater than the mechanical chopper period T, so that it was possible to observe a smooth excitation profile of the fluorescence, and this time constant exceeded the characteristic scanning time of the line profile took place. An important feature of the experiments was the selection of the temperature of the source of the main atomic beam. As pointed out in Sec. 2, the only transition by which the fluorescence could be generated in the probe field was $F = 2 - F' = 3$. However, the separation between the $F' = 3$ and $F' = 2$ sublevels of the excited states was only 60 MHz and the width of the emission spectrum of the probe laser was 20 MHz, so that the probe laser could induce transitions of atoms from the $F = 2$ to the $F' = 2$ level followed by spontaneous decay to the $F = 1$ level. This effect resulted in a strong reduction in the concentration of the atoms at the $F = 2$ sublevel in the region where the fluorescence was recorded and it also produced a strong reduction in the intensity of the fluorescence due to the probe beam, which fell below the sensitivity threshold of the recording apparatus. The simplest method for increasing the fluorescence intensity was an increase in the temperature of the atomic beam source, which should increase the total concentration of atoms. However, an increase in this concentration in a beam gave rise to the formation of an optically dense layer in the interaction zone and this reduced the distance of the zone of interaction with the strong field.

Preliminary experiments showed that the optimal temperature was $t = 300$°C. At this temperature the attenuation of the radiation due to the high concentration near the source was slight and fluorescence due to the probe beam could be recorded quite reliably. One should point out that at the selected working temperature of the source and for the selected the exit diameter of the source aperture, the flow of atoms out of the source was effusive.

4. EXPERIMENTS AND RESULTS

The main experimental problem was the need for careful control of the uniformity of the scanning of the probe laser frequency along the absorption profile of the atomic beam. Sudden changes in the probe laser frequency could give rise to sharp peaks in the fluorescence profile and these were due to the interaction between the laser radiation and a new group of atoms in an inhomogeneously broadened Doppler profile of the absorption line. These stray effects were discriminated against by monitoring the uniformity of the laser scanning frequency using an additional cell with sodium vapor, and also using the main atomic beam when the strong field was switched off. By way of example, Fig. 6(a) shows an oscillogram of the fluorescence line profile of atoms in the main atomic beam when the strong laser beam was switched off. This oscillogram is a smooth contour without characteristic peaks and the dips.

Another preliminary experiment carried out to check the stability of the strong laser frequency involved

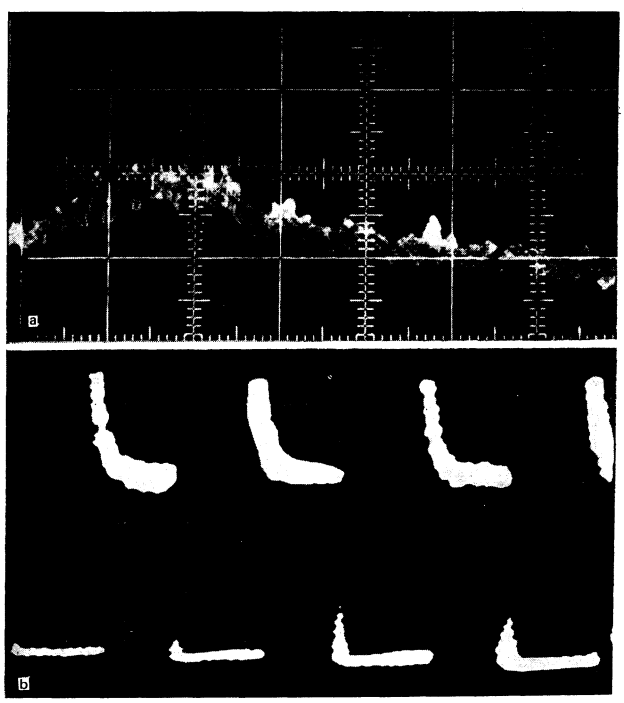

FIG. 6. a) Profile of a fluorescence line of the Na atoms in the main beam when the strong laser beam is switched off. b) Oscillogram of the dependence of the fluorescence signal of the sodium atoms at the point $z = 40$ cm on the duration of irradiation of the atomic beam with the strong field alone. One division along the horizontal scale corresponds to 2 msec.

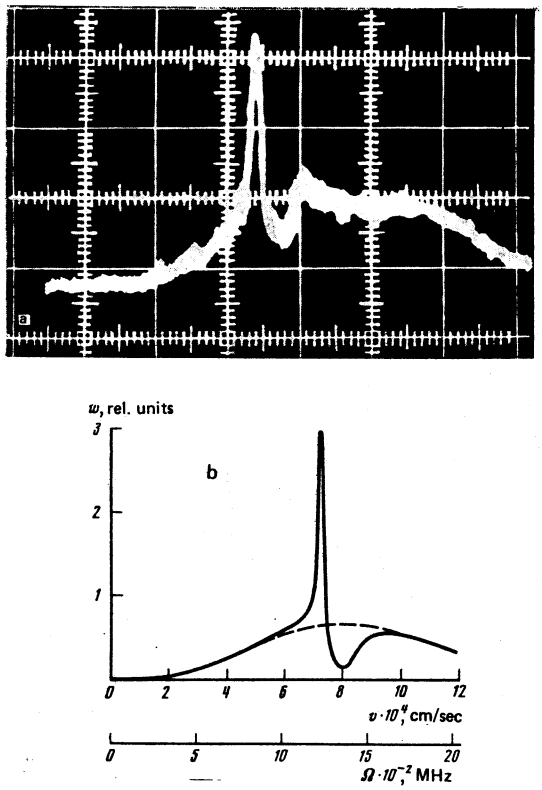

FIG. 7. a) Experimental profile of a deformed velocity distribution corresponding to $G=40$ (one horizontal division is 220 MHz). b) Calculated dependence of the deformation of the velocity distribution.

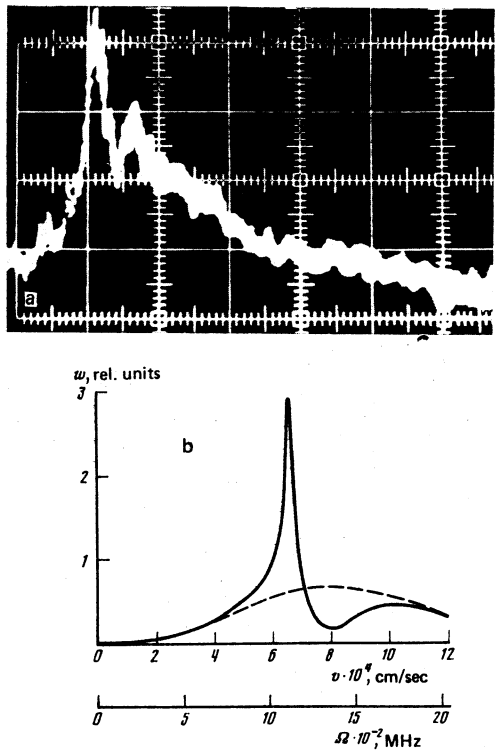

FIG. 8. a) Experimental profile of a deformed velocity distribution corresponding to $G=320$ (one horizontal division in Fig. 8a is 440 MHz).

recording the time dependence of the fluorescence signal due to the strong beam when the weak beam was switched off [Fig. 6(b)]. The fluorescence signal was then proportional to the number of atoms with the resonance velocity v_{res} (Fig. 1) and was a falling function of time (see Ref. 6). The absence of sharp peaks in this dependence demonstrated stability of the emission frequency of the strong laser.

The sequence of the experiments was as follows. A strong laser beam was injected into a vacuum chamber containing an active atomic beam and the two beams were collinear. A mechanical chopper 14 switched on the laser radiation for a time longer than the transit time of an atom across the interaction zone. Scanning of the strong-field frequency over the fluorescence signal was tuned to the D_2 absorption line of sodium atoms. Combination of the frequencies of two axial modes with two absorption profiles of sodium atoms (Figs. 3 and 4) was achieved on the basis of the observation of a characteristic fall of the fluorescence signal on increase in the duration of interaction of atoms with laser radiation [Fig. 6(b)]. Then, the fluorescence generated in this strong field was interrupted by another chopper with a period T (see Fig. 3) and at the same time the probe radiation, used to record the fluorescence signal, was injected into the chamber.

Typical experimental dependences of the fluorescence intensity on the frequency of the probe laser beam are shown in Figs. 7(a) and 8(a). Figure 7(a) corresponds to the saturation parameter of just one mode $G=I/I_{sat}=40$. Figure 8(a) corresponds to $G=320$ ($I_{sat}=10$ mW/cm^2). The frequency of the strong beam was in both cases tuned to the absorption line maximum. The oscillograms obtained indicated that the velocity distribution was characterized by two features. Firstly, the distribution had a dip near the resonance velocity. Secondly, in the region of slower velocities there was a narrow peak corresponding to the atoms which were slowed down.

The frequency scale was calibrated using the dependences of the fluorescence intensity on the frequency of the probe laser obtained by directing the laser beam at right-angles to the beam of sodium atoms. The two peaks in the fluorescence spectrum corresponded to the two levels $F=1$ or 2 of the ground state $3S_{1/2}$ and the frequency difference between these levels was 1772 MHz. Using this interval as the calibration measure of the frequency scale, we determined the parameters of the velocity distribution. For the $G=40$ case [Fig. 7(a)] the width of the peak was 70 MHz and the shift of the maximum of the velocity distribution was 150 MHz. At a higher laser radiation intensity corresponding to $G=320$ [Fig. 8(a)] the maximum shifted by a larger interval of 250 MHz and the width of the peak also increased to 190 MHz when the radiation intensity rose. The broadening of the peak, observed on increase in the intensity, was in qualitative agreement with the results of a numerical calculation.[13] On the frequency scale the width of the peak in Fig. 7(a) was $\Delta v=\lambda\Delta\nu=4.1\cdot10^3$ cm/sec, and that peak in Fig. 8(a) was 1.1×10^4 cm/sec. Using these values we could find the relative monochromatization of the atomic beam, which

was defined as the ratio of the width of the initial velocity distribution to the width of the resultant peak. In the former case the degree of monochromatization μ was 19, whereas in the latter case it was 7.

5. COMPARISON WITH A THEORY

The main reason for the deformation of the longitudinal-velocity distribution of an atomic beam is the action of the optical pressure force on the atoms. In view of the nonlinear (Lorentzian) dependence of this force on the velocity, it slows down most effectively those atoms whose velocities are close to the resonance value $v_{res} = -\Omega/k$. Consequently, the optical pressure force produces a velocity dip at $v \approx v_{res}$ and a corresponding velocity peak at velocities less than the resonance value v_{res} (see Fig. 1). Another important factor which governs the motion of atoms is the velocity diffusion. This diffusion broadens a narrow peak of the slowed-down atoms in the velocity distribution as time increases. Therefore, the experimentally observed deformation of the velocity distribution should be due to two factors: narrowing under the action of the optical pressure force and diffusion broadening.[13] Consequently, an exact quantitative description of a deformed velocity distribution can be obtained starting from a suitable Fokker–Planck equation,[14,15] which allows for the optical pressure force and for the velocity diffusion effect.

We shall estimate the contribution of the force and of the velocity diffusion to the experimentally observed deformation of the velocity distribution. We shall do this by noting first that since two laser waves excite all the hyperfine structure levels $F' = 0$, 1, 2, and 3 of the upper state $3P_{3/2}$, the characteristic frequency width of the force and diffusion are given (to within an order of magnitude) by the width of the upper level $\Delta\nu \approx 100$ MHz (Fig. 3). We shall now determine the distance l_{res} in which the force shifts atoms out of their resonance with the light waves. Clearly, the distance l_{res} can be found from the condition of the shift of the velocity distribution maximum by $\Delta\omega/k$:

$$F\tau_{res}/M \approx \Delta\omega/k, \tag{1}$$

where the time τ_{res} in the case of a practically constant atomic velocity $v_{res} \approx -\Omega/k$ is proportional to the length l_{res}:

$$\tau_{res} \approx l_{res}/v_{res}. \tag{2}$$

It follows from Eqs. (1) and (2) and from the order of magnitude of the force $F \approx \hbar k\gamma$ that

$$l_{res} \approx \lambda\!\!\!^{-}(\Delta\omega/\gamma)(v_{res}/v_{rec}), \tag{3}$$

where $\lambda\!\!\!^{-} = \lambda/2\pi$ and $v_{rec} = \hbar k/M$. Substituting the value $v_{res} = 8\times10^4$ cm/sec (which is the velocity at the maximum of the initial distribution), we find that $l_{res} \approx 5$ cm. Although the slowing-down distance (length) used in the experiments was 20 cm, it follows from our estimate that the force should deform considerably the velocity distribution.

We shall now estimate the diffusion broadening of the velocity distribution in the slowing-down distance $l = 20$ cm:

$$\Delta v_d \approx (D\tau_d)^{1/2}, \tag{4}$$

where D is the velocity diffusion coefficient. Since over a distance of 20 cm we can still ignore the changes in the velocity, it follows that τ_d can be estimated from

$$\tau_d = l/v_{res}. \tag{5}$$

We shall assume that the diffusion coefficient is the maximum value $D = \gamma v_{rec}^2$, in which case we can only overestimate the diffusion broadening. It then follows from Eqs. (4) and (5) that the upper limit to the diffusion broadening of the velocity peak is

$$\Delta v_d \approx v_{rec}(\gamma l/v_{res})^{1/2}. \tag{6}$$

For $l = 20$ cm and $v_{res} = 8\times10^4$ cm/sec, we find that Eq. (6) gives $\Delta v_d \approx 300$ cm/sec. On the frequency scale the upper estimate of the diffusion broadening is $\Delta\nu_d = \Delta v_d/\lambda \approx 5$ MHz. Since even the upper limit to the diffusion broadening is much less than the broadening due to the optical pressure force, we may conclude that the diffusion of the atomic velocities plays no significant role in the experiments of the kind described above. Consequently, the main contribution to the experimentally observed deformation of the velocity distribution is made by the optical pressure force.

We can calculate the deformation of the velocity distribution under the action of the optical pressure force F by replacing the Fokker–Planck equation with the simpler Liouville equation for the distribution function $w(\mathbf{r}, \mathbf{v}, t)$:

$$\frac{\partial w}{\partial t} + \mathbf{v}\frac{\partial w}{\partial \mathbf{r}} = -\frac{\partial}{\partial \mathbf{p}}(\mathbf{F}w). \tag{7}$$

In the determination of the force F we can replace a complex multilevel scheme of the sodium atom [Fig. 3(a)] by a simpler three-level scheme [Fig. 3(b)]. In this equivalent scheme the two lower levels correspond to the $F = 1$ and 2 levels of the ground state $3S_{1/2}$, and the uppermost level with an effective width $\Delta\nu = 100$ MHz represents all the levels $F' = 0, 1, 2, 3$ of the upper state $3P_{3/2}$.

The exact expression for the optical pressure force in the case of a three-level atomic system in which the width of the upper level is entirely due to spontaneous decay to the two lower levels is obtained in Ref. 16. In the situation in our experiments when the difference between the frequencies of two laser modes is identical with the frequency interval between the two lower levels ($\nu_{L2} - \nu_{L1} = \Delta = 1772$ MHz) and the detunings $\Omega_1 = \nu_{L1} - \nu_{01} = \Omega$, and $\Omega_2 = \nu_{L2} - \nu_{02} = \Omega$ do not agree with the interval Δ ($\Delta - |\Omega| \gg \gamma$), the optical pressure force is[16]

$$F = -\hbar k\gamma \frac{2G}{2 + [(\Omega + kv)^2/\gamma^2 + 3/2]G}, \tag{8}$$

where $2\gamma = 10$ MHz is the radiative width of the transition under consideration and $G = G_1 = G_2$ is the saturation parameter for one laser wave.

We can obtain the force from Eq. (8) for the equivalent three-level system with an effective width of the upper level $\Delta\omega$ by writing down the detuning in the form $\Omega = \bar{\Omega} + \omega'$ and averaging Eq. (8) over the frequen-

cy ω' within the limits of the effective width $\overline{\Delta\omega}$ (in the interval $-\Delta\omega/2 \leq \omega' \leq \Delta\omega/2$):

$$F=\frac{1}{\Delta\omega}\int_{-\Delta\omega/2}^{+\Delta\omega/2} F\,d\omega'$$
$$=-\hbar k\gamma\frac{G}{(2+{}^3/_2G)^{1/2}}\frac{\gamma}{\Delta\omega}\operatorname{arctg}\frac{2\gamma\Delta\omega(2+{}^3/_2G)^{1/2}}{(2+{}^3/_2G)\gamma^2+(\Delta\omega)^2+(\overline{\Omega}+kv)^2}. \quad (9)$$

In the final expression (9) the quantity $\overline{\Omega}$ is the average detuning related to the center of the upper level. One should point out that since the levels of the hyperfine structure of the upper state $3P_{3/2}$ are replaced with the fine-structure level $3P_{3/2}$ in the investigated equivalent three-level system, G in Eq. (9) represents the saturation parameter of the $3S_{1/2}(F=1)-3P_{3/2}$ transition or of the $3S_{1/2}(F=2)-3P_{3/2}$ transition. The saturation intensities for these transitions are equal and have the numerical value $I_{sat}=10$ mW/cm^2.

Using Eq. (9), we find that the Liouville equation describing the evolution of the longitudinal-velocity distribution $w(z,v,t)$ is

$$\frac{\partial w}{\partial t}+v\frac{\partial w}{\partial z}+\frac{\partial}{\partial p}(\bar{F}w)=0. \quad (10)$$

The only indeterminate parameter in Eq. (10) remains the width of the upper level $\Delta\omega$. In order to find $\Delta\omega$, we compared the experimentally observed fall of the fluorescence intensity with time [Fig. 6(b)] with that predicted on the basis of a numerical solution of Eq. (10) for different parameters $\Delta\omega$. Since the fluorescence intensity at the point $z=l$ is proportional to the expression[6]

$$I_{fl}(z=l,t)\propto\int w(z=l,v,t)\bar{F}(v)\,dv, \quad (11)$$

we find by solving Eq. (10) and comparing Eq. (11) with the experimental curves [Fig. 6(b)], that the best agreement is obtained for $\Delta\omega=60$ MHz. This value is slightly smaller than $\Delta\omega=70$ MHz found earlier.[6]

The calculated dependences of the distribution of atoms on their velocity are plotted in Fig. 7(b) and 8(b) for the values $G=40$ and $G=320$ used in the experiments. The dashed curve in these figures is the initial velocity distribution at 573 K. The curves obtained are not only in good qualitative agreement with the experimental dependences, but they also give the shift of the velocity distribution maximum close to that found in the experiments. For example, if $G=40$, the theoretical shift is 130 MHz (the experimental shift is 150 MHz), whereas for $G=320$ the theoretical shift 240 MHz is even closer to the experimental 250 MHz.

The widths of the calculated peaks are several times narrower than those observed experimentally. Since the velocity diffusion cannot be significant in the experiments described earlier, we may assume that the disagreement between the experimental and calculated widths is due to the employment of an insufficiently accurate expression for the optical pressure force. The force of Eq. (9) contains one maximum at the velocity $v\approx-\Omega/k$. The exact force should have four maxima corresponding to transitions from each of the lower states $F=1$ or 2 to the four upper states $F'=0,1,2,3$. Since each maximum of the force gives rise to its own velocity peak, the positions of the four velocity peaks may give rise to an additional resultant peak.

6. CONCLUSIONS

It was found that in a short effective interaction length of 20 cm the optical pressure deformed effectively approximately one-tenth of the atoms from their initial distribution. The average velocity for this group of atoms was reduced from 8×10^4 cm/sec ($T_{in}=573$ K) to 7.1×10^4 cm/sec. The narrowing of the velocity distribution compared with the initial thermal distribution was $\mu=19$ ($G=40$). This corresponded to lowering of the relative temperature of the atoms from $T_{in}=573$ K to $T_{fin}=T_{in}/\mu^2=1.5$ K.

We point out finally that in view of the reasonable agreement between the experimental and calculated velocity distributions, and using the theoretical predictions of Ref. 11, we can expect that a complete slowing down of a significant part of the thermal beam of sodium atoms can be achieved simply by increasing the interaction length to a value of about 100 cm.

[1]R. Schieder, H. Walther, and L. Wöste, Opt. Commun. **5**, 337 (1972).
[2]A. F. Bernhardt, D. E. Duerre, J. R. Simpson, and L. L. Wood, Opt. Commun. **16**, 169 (1976).
[3]J. E. Bjorkholm, R. R. Freeman, A. Ashkin, and D. B. Pearson, Phys. Rev. Lett. **41**, 1361 (1978).
[4]E. Arimondo, H. Lew, and T. Oka, Phys. Rev. Lett. **43**, 753 (1979).
[5]V. I. Balykin, V. S. Letokhov, and V. I. Mishin, Pis'ma Zh. Eksp. Teor. Fiz. **29**, 614 (1979) [JETP Lett. **29**, 560 (1979)]; Zh. Eksp. Teor. Fiz. **78**, 1376 (1980) [Sov. Phys. JETP **51**, 692 (1980)].
[6]V. I. Balykin, V. S. Letokhov, and V. G. Minogin, Zh. Eksp. Teor. Fiz. **80**, 1779 (1981) [Sov. Phys. JETP **53**, 919 (1981)].
[7]V. S. Letokhov and V. G. Minogin, Phys. Rep. **73**, 1 (1981).
[8]I. V. Krasnov and N. Ya. Shaparev, Zh. Eksp. Teor. Fiz. **77**, 899 (1979) [Sov. Phys. JETP **50**, 453 (1979)].
[9]I. V. Krasnov and N. Ya. Shaparev, Zh. Eksp. Teor. Fiz. **79**, 391 (1980) [Sov. Phys. JETP **52**, 196 (1980)].
[10]V. G. Minogin, V. S. Letokhov, and T. V. Zueva, Opt. Commun. **38**, 225 (1981).
[11]T. V. Zueva, V. S. Letokhov, and V. G. Minogin, Zh. Eksp. Teor. Fiz. **81**, 84 (1981) [Sov. Phys. JETP **54**, 38 (1981)].
[12]I. V. Hertel and A. S. Stamatovic, IEEE J. Quantum Electron. **QE-11**, 210 (1975).
[13]V. G. Minogin, Opt. Commun. **34**, 265 (1980).
[14]V. G. Minogin, Zh. Eksp. Teor. Fiz. **79**, 2044 (1980) [Sov. Phys. JETP **52**, 1032 (1980)].
[15]R. J. Cook, Phys. Rev. A **22**, 1078 (1980).
[16]V. G. Minogin and Yu. V. Rozhdestvenskiĭ, Opt. Spektrosk. (in press).

Translated by A. Tybulewicz